

Interferometric Signatures of Single Molecules

Taras Plakhotnik* and Viktor Palm†

Physical Chemistry Laboratory, Swiss Federal Institute of Technology, ETH-Zentrum, CH-8092 Zurich, Switzerland
(Received 19 March 2001; published 15 October 2001)

We built an interferometer where one of the two slits of a classical Young's setup is replaced by a single molecule embedded in a solid matrix. This enabled direct measurement of the first order coherence of the 0-0 single-molecule emission, which at high excitation powers proves to be split in coherent and incoherent parts. We demonstrate an order of magnitude higher precision in axial localization of single molecules in comparison with that of confocal microscopy. These experiments open a possibility for single-molecule holography. Detection of single molecules with low luminescence quantum yields could be another application of this technique.

DOI: 10.1103/PhysRevLett.87.183602

PACS numbers: 42.50.Ar, 32.50.+d, 42.25.Hz, 42.40.Kw

Since the pioneering experiments of Young [1], interference remains one of the most spectacular phenomena in optics and a very informative approach. However, although characterization and manipulation of individual molecules has developed into a powerful tool [2–7], relevant optical methods on a single-molecule (SM) level are practically limited to the detection of Stokes shifted luminescence. Conventionally, a SM is excited by a laser but to protect a photodetector from the laser light, a cutoff filter is used which also blocks the unshifted SM emission. A general belief that SM absorption [8,9] provides a smaller signal-to-noise ratio (SNR) and should be based on complex modulation techniques to be competitive has created a psychological barrier for all methods where a cutoff filter does not block off the laser radiation. Our Letter shows that existing beliefs are limited and that SM interferometry can give an excellent SNR. This opens new options for SM applications and gives us a new tool for fundamental studies.

The experimental setup is shown in Fig. 1 and is explained in the figure caption. A key element of the setup is the aperture A whose diameter is smaller than the diffraction limited spot size into which the lens L_2 focuses SM emission. Such an aperture blocks a part of the reference beam not overlapping the SM emission and removes phase inhomogeneities in the two beams caused by optical imperfections. The overlapping parts of the reference and signal beams result in interference. This becomes evident when the count rate of the photomultiplier (PM) is recorded as a function of the laser frequency which is scanned across a SM resonance. Three examples of interferograms are shown in Fig. 2. As demonstrated in Fig. 3, the interference patterns become smaller in the relative amplitude and broader in frequency at higher excitation laser powers.

Only emission with a frequency equal to the frequency of the laser light contributes to the interferograms, whereas SM emission falling on the aperture has a complex spectrum which includes a resonance 0-0 line and a set of Stokes shifted vibronic lines. All lines are accompanied also by Stokes shifted phonon wings [10]. The intensity of the 0-0 emission under resonance laser excitation

is given by a count rate R_0 of the PM. Based on the luminescence spectra and the count rate measured with a red filter inserted behind the aperture (this gives the integrated intensity of the luminescence with a wavelength longer than 610 nm), we estimate that $R_0 \approx 10$ Hz under excitation by 2 nW radiation. At this power, the laser beam passing through the aperture produces a count rate $R_{\text{ref}} \approx 25$ kHz. At low laser powers $R_0 \propto R_{\text{ref}}$ and we

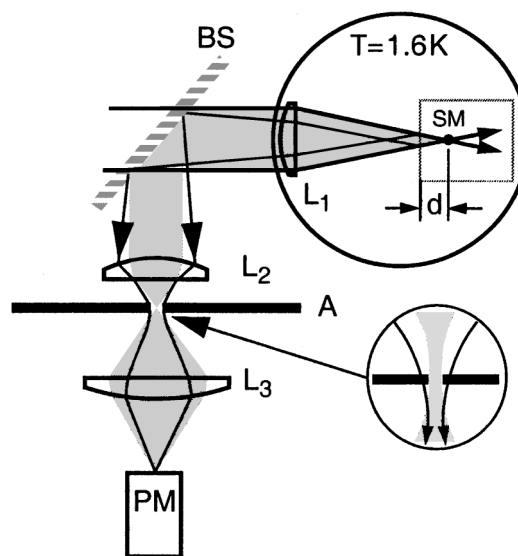


FIG. 1. Experimental setup. A naphthalene crystal (represented by the rectangle) doped with terylene molecules is placed in an optical cryostat at a temperature of 1.6 K. A microscope objective L_1 (Newport M-60 \times , NA = 0.85) focuses the laser light of approximately 574 nm wavelength generated by a single mode dye laser into an approximately Gaussian spot with a full width at half maximum of 1.6 μm . The same objective collects and collimates the emission (shown in grey) of a SM. The collimated beam has a diameter of ~ 4 mm. A weak reflection ($\sim 4\%$ of the incoming laser power) from the front surface of the crystal plays the role of a reference beam. The molecular emission is focused by the lens L_2 ($F = 80$ mm) into the aperture A of 10 μm diameter. Lens L_3 focuses the light passing through the aperture onto a PM. d is the distance from a SM to the crystal surface. BS labels a beam splitter.

designate the low power ratio $\sqrt{R_0/R_{\text{ref}}}$ by A_0 . In our experiments $A_0 \approx 0.02$.

We first analyze the interference at low laser powers. At 1.6 K, the low power 0-0 linewidth Γ_0 (half width at half maximum) of a terrylene molecule doped in a naphthalene crystal is only about 15% broader than the lifetime-limited value Γ_τ [11], indicating that pure dephasing caused by the matrix [12] is small. Therefore, we consider SMs as simple classical damped oscillators driven by a classical electromagnetic field (whose frequency and vacuum wavelength are ω and λ , respectively). The reflected laser field E_{ref} ($|E_{\text{ref}}|^2 \propto R_{\text{ref}}$) and the field E_m emitted by a SM ($|E_m|^2 \propto R_0 \mathcal{L}(\omega)$, where $\mathcal{L}(\omega)$ is a Lorentzian line-shape function) create the total field [13]

$$E_{\text{tot}} = \alpha \left[\sqrt{R_{\text{ref}}} e^{i\varphi} + \sqrt{R_0} \frac{\Gamma_0}{(\omega - \omega_0) + i\Gamma_0} \right], \quad (1)$$

where α is a constant which matches units of the two sides and ω_0 is the SM resonance frequency. $\varphi = \varphi_0 - 4\pi nd/\lambda$, where φ_0 is a constant and $4\pi nd/\lambda$ is the phase shift between the molecular emission and the reference laser beam caused by the difference $2d$ in the corresponding path lengths, as shown in Fig. 1 ($n \approx 1.5$ is the refractive index of the crystal). The PM count rate $R(\omega) \propto |E_{\text{tot}}|^2$ reads

$$R(\omega) = \left[1 - 2A_0\Gamma_0 \times \frac{\Gamma_0 \sin \varphi + (\omega_0 - \omega) \cos \varphi}{\Gamma_0^2 + (\omega - \omega_0)^2} \right] B(\omega). \quad (2)$$

$B(\omega)$ is the base line of the laser intensity in the absence of the molecule. This base line was not flat but had a cosine modulation (probably created by interference on the optical elements or by a small displacement of the laser beam across the aperture as the laser frequency was scanned). The depth of this modulation was comparable with the effect caused by a SM ($\sim 3\%$) but its period was approximately 3.5 GHz while the molecular linewidth was 2 orders of magnitude smaller. The base line in Eq. (2) was fitted together with the part depending on the SM. In Fig. 2 both the experimental signal and the fit were divided by $B(\omega)$. In each case, Γ_0 and ω_0 were independently determined from the SM excitation spectra [14]. Such measurements were made by introducing a red cutoff filter in front of the PM.

A dramatic difference between interferograms shown in Figs. 2(a) and 2(b) results from a difference of $\delta\varphi = 0.58\pi$ between the corresponding phase shifts. The related difference in the locations of the two molecules with respect to the crystal surface δd is $\lambda\delta\varphi/(4\pi n) \approx \lambda/10 \approx 55$ nm. In SM confocal microscopy [15], an axial displacement of more than λ is needed to obtain a maximum of the signal instead of a “zero.” Consequently, the highest axial accuracy of single-molecule localization achieved so far with far-field optics was 100 nm [16]. Figures 2(b) and 2(c) clearly demonstrate the effect of a tiny 14(3) nm

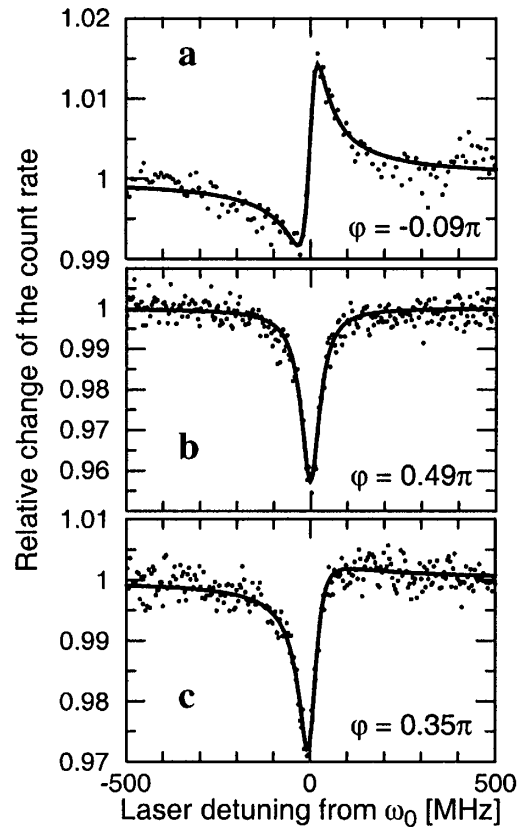


FIG. 2. Three examples of the relative change of count rate (dots) as a function of laser frequency detuning when the laser frequency is close to the resonance frequency of an electronic transition. The phase shifts are determined from the fits to Eq. (2) (solid lines). Data are normalized by the base-line count rate. The magnitude of variations of the base line is indicated in Fig. 3. The laser power was 2 nW.

displacement. Our technique also does not require time consuming axial scanning, in contrast with confocal microscopy. From an interferogram, the SM position can be determined up to a multiple of $\lambda/(2n)$. If necessary, confocal microscopy which has a precision better than $\lambda/(2n)$ can be used to eliminate this uncertainty.

At high laser powers, the peak intensity of the excitation line and the linewidth saturate. The saturation parameter $\xi = P/P_s$, where $P \propto R_{\text{ref}}$ is the laser power and P_s is the saturation power. The peak intensity and the linewidth change according to $R_0 = R_\infty \xi / (1 + \xi)$ and $\Gamma_s = \Gamma_0 \sqrt{1 + \xi}$, respectively [12]. Naively, one can try Eqs. (1) and (2) at high powers by substituting Γ_s for Γ_0 in the line-shape function and taking the saturated value for R_0 (note that $\sqrt{R_0/R_{\text{ref}}} = A_0 \Gamma_0 / \Gamma_s$). This leads to

$$R(\omega) = \left[1 - 2A_0\Gamma_0 \times \frac{\Gamma_s \sin \varphi + (\omega_0 - \omega) \cos \varphi}{\Gamma_s^2 + (\omega - \omega_0)^2} \right] B(\omega). \quad (3)$$

Fits to Eq. (3) are shown in Fig. 3 by the grey lines. Essentially, only the base lines were fitted. Parameters

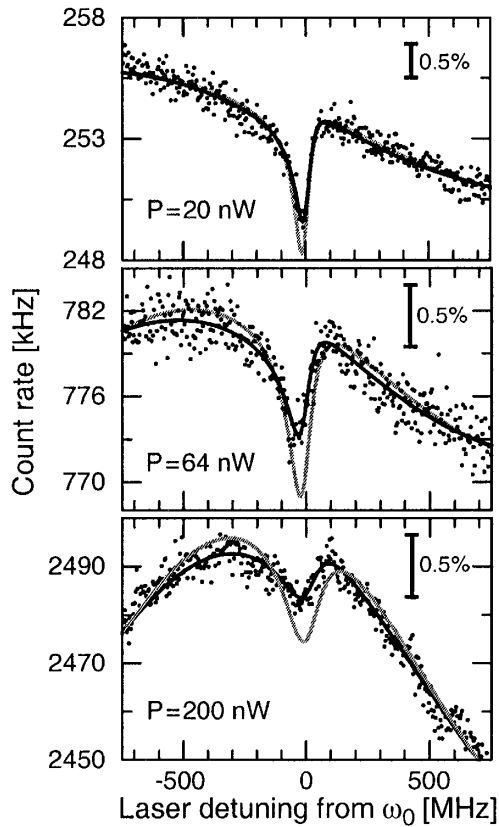


FIG. 3. The dependence of the line shown in Fig. 2(c) on the laser power. The dots represent experimental data and the vertical bars are equal to 0.5% of the base-line level. The black solid lines are the quantum electrodynamic prediction given by Eq. (4). The standard deviations of the experimental points from the corresponding theoretical curves is only 10% larger than the shot noise limit. The grey solid lines are the fits to Eq. (3) which assume that all SM 0-0 emission is coherent. The base line was fitted but, in contrast to Fig. 2, the data were not normalized by $B(\omega)$.

$A_0 = 0.018$ and $\varphi = 0.35\pi$ were determined from the low power measurements. The unsaturated linewidth $\Gamma_0 = 26$ MHz and the saturation power $P_s = 17.8$ nW were determined from excitation spectra. Evidently, the data deviate significantly at high laser powers from Eq. (3). The reason for this deviation is that at strong excitation the resonance fluorescence consists of coherent and incoherent parts. The total intensity R_0 is a sum of the two contributions. But only the coherent part can interfere with the laser emission. The incoherent part is related to a fluorescence triplet (Mollow triplet) [17,18] of a strongly driven two-level system. The coherent part is related to an elastic component of the fluorescence spectrum and gradually goes to zero when the laser power approaches infinity.

The following analysis is based on quantum electrodynamics. When fields are described by operators, $R(\omega) \propto \langle \hat{E}_{\text{ref}}^- \hat{E}_{\text{ref}}^+ \rangle + 2\text{Re}(\langle \hat{E}_{\text{ref}}^- \hat{E}_m^+ \rangle) + \langle \hat{E}_m^- \hat{E}_m^+ \rangle$. The first term is the intensity of the laser beam, the last term is the 0-0 fluorescence intensity which has a negligible relative magnitude, and the middle term is the interference

term. A coherent laser field can be treated classically. The expectation value for the molecular field $\langle \hat{E}_m^+ \rangle$ is equal to the field emitted by an oscillating dipole $\mu \rho_{12}(t)$ [19], where μ is the 0-0 transition dipole moment. The density matrix element ρ_{12} is the steady-state solution of the optical Bloch equations [19]. These equations can also account for the pure dephasing caused by interaction with the matrix and for the fact that an organic molecule has not only the ground and excited singlet electronic states (states 1 and 2) but also vibrational and triplet states (see, for example, [20]). The expression for $R(\omega)$ obtained in this way reads

$$R(\omega) = \left[1 - 2A_0\Gamma_0 \times \frac{\Gamma_0 \sin\varphi + (\omega_0 - \omega) \cos\varphi}{\Gamma_s^2 + (\omega - \omega_0)^2} \right] B(\omega). \quad (4)$$

The interference term in Eq. (4) is $\sqrt{1 + \xi}$ times smaller at exact resonance in comparison with that of Eq. (3) due to Γ_0 in the numerator. In Eqs. (4) and (3), the coefficient A_0 should be multiplied by $\sqrt{\Gamma_\tau/\Gamma_0}$ if the pure dephasing contribution to Γ_0 is essential. But this makes no difference to fitting, where A_0 is considered simply as a fit parameter. The quantum electrodynamic model, whose predictions are given by the black lines in Fig. 3, fits the data significantly better than Eq. (3). Decoherence of the resonance emission by a strongly driven quantum system was not observed in earlier interference experiments done on ions in a Pauli trap [21] only under nonsaturating conditions.

In principle, the time needed to achieve a certain level of SNR in the interference experiment described above is independent of the reference beam intensity, provided that the signal noise is dominated by the shot noise. Indeed, the variation of $R(\omega)$ across a SM resonance is proportional to $2t_m\sqrt{R_{\text{ref}}R_0}$, while the quantum noise of the signal is $\sqrt{t_m R_{\text{ref}}}$, where t_m is the measuring time. It follows that $\text{SNR} \propto 2\sqrt{t_m R_0}$. However, a weak reference beam increases the relative magnitude of the interference effect while increasing quantum noise by decreasing the count rate. In practice, this significantly relaxes the requirements for the laser intensity stability, and allows us to demonstrate a SNR which could be achieved only in ideal absorption measurements.

Whether interferometry or detection of Stokes luminescence gives a better SNR is a nontrivial question. The SNR in interferograms and in background-free excitation spectra is equal to $2\sqrt{\Gamma_\tau\Gamma_0^{-1}t_m R_0/(1 + \xi)}$ and $\sqrt{(\phi^{-1} - 1)t_m R_0}$, respectively, where ϕ is the relative intensity of the 0-0 line in the luminescence spectrum. In the second expression, we assume that the cutoff filter suppresses only the 0-0 line but is 100% transparent for the Stokes shifted luminescence. Neither of the two methods has a clear advantage if $\Gamma_0 \approx \Gamma_\tau$. In the case of a strong 0-0 line and weak

vibronic lines, interferometry can be a better choice. Moreover, $P_s \propto \Gamma_r \Gamma_0 / (\phi \Gamma_r)$ [12] and, at a low luminescence quantum yield when the radiative linewidth $\Gamma_r \ll \Gamma_\tau$, high laser powers are needed for a good SNR. In practice, this results in a high background (e.g., luminescence from the matrix), a case when interferometry provides a better SNR. Usually weakly dependent on the laser frequency, background does not disturb interferograms if the reference laser signal is stronger than this background. In our experiments, the intensity of SM emission was 2500 times weaker than that of the reference beam. If broadband luminescence of the matrix were 500 times stronger than the peak intensity of the SM line (but still 5 times weaker than the reference beam), this would be practically fatal for excitation spectra (2200% noise increase) but would increase the noise in interferograms by $\sim 10\%$.

Besides being of fundamental interest, opening a practical possibility for high precision SM localization and for spectroscopy of single molecules whose emission is obscured by a strong background signal, our experiments also make holography of single molecules a realistic perspective. To obtain a hologram, a photomultiplier should be replaced by a CCD camera, and a 2-dimensional interference pattern is recorded.

This work was financially supported by the ETH-Zurich.

*Corresponding author.

Email address: taras@phys.chem.ethz.ch

†Permanent address: Institute of Physics, University of Tartu, 51014 Tartu, Estonia.

- [1] See, e.g., M. Born and E. Wolf, *Principles of Optics* (Pergamon, London, 1959).
- [2] W. E. Moerner and M. Orrit, *Science* **283**, 1670 (1999).
- [3] S. Weiss, *Science* **283**, 1676 (1999).
- [4] J. K. Grimzewski and C. Joachim, *Science* **283**, 1683 (1999).
- [5] A. D. Mehta *et al.*, *Science* **283**, 1689 (1999).
- [6] X. S. Xie and J. K. Trautman, *Annu. Rev. Phys. Chem.* **49**, 441 (1998).
- [7] P. Tamarat, A. Maali, B. Lounis, and M. Orrit, *J. Phys. Chem. A* **104**, 1 (2000).
- [8] W. E. Moerner and L. Kador, *Phys. Rev. Lett.* **62**, 2535 (1989).
- [9] L. Kador, T. Latychevskaia, A. Renn, and U. P. Wild, *J. Chem. Phys.* **111**, 8755 (1999).
- [10] K. K. Rebane, *Impurity Spectra of Solids* (Plenum, New York, 1970).
- [11] E. A. Donley, V. Burzomato, U. P. Wild, and T. Plakhotnik, *J. Lumin.* **83–84**, 255 (1999).
- [12] W. P. Ambrose, Th. Basché, and W. E. Moerner, *J. Chem. Phys.* **95**, 7150 (1991).
- [13] J. D. Jackson, *Classical Electrodynamics* (Wiley, New York, 1999).
- [14] M. Orrit and J. Bernard, *Phys. Rev. Lett.* **65**, 2716 (1990).
- [15] R. H. Webb, *Rep. Prog. Phys.* **59**, 427 (1996).
- [16] A. M. Van Oijen, J. Köhler, J. Schmidt, M. Müller, and G. J. Brakenhoff, *Chem. Phys. Lett.* **292**, 183 (1998).
- [17] B. R. Mollow, *Phys. Rev.* **188**, 1969 (1969).
- [18] F. Y. Wu, R. E. Grove, and S. Ezekiel, *Phys. Rev. Lett.* **35**, 1426 (1975).
- [19] R. Loudon, *The Quantum Theory of Light* (Oxford, New York, 1983).
- [20] H. de Vries and D. A. Wiersma, *J. Chem. Phys.* **72**, 1851 (1980).
- [21] U. Eichmann *et al.*, *Phys. Rev. Lett.* **70**, 2359 (1993).